Dosimetry of ^{188}Re-Hydroxyethylidene Diphosphonate in Human Prostate Cancer Skeletal Metastases

Knut Liepe, MD[1]; Reiner Hliscs, PhD[1]; Joachim Kropp, MD[1]; Roswitha Runge[1]; Furn F. (Russ) Knapp, Jr., PhD[2]; and Wolf-Gunter Franke, MD[1]

[1]Department of Nuclear Medicine, University Hospital Dresden, Dresden, Germany; and [2]Nuclear Medicine Group, Oak Ridge National Laboratory, Oak Ridge, Tennessee

^{188}Re-Hydroxyethylidene diphosphonate (^{188}Re-HEDP) was used in previous studies for the palliative treatment of metastatic bone pain. However, the kinetic and radiation-absorbed doses have not been well documented. Therefore, the aim of this study was to gather dosimetric data for ^{188}Re-HEDP. **Methods:** Thirteen prostate cancer patients with skeletal involvement were treated with 2,700–3,459 MBq (mean dose, 3,120 MBq) ^{188}Re-HEDP. Patients underwent whole-body scans 3, 20, and 28 h after therapy. The effective half-life, residence time, and radiation-absorbed dose values were calculated for the whole body, bone marrow, kidneys, and bladder as well as for 29 bone metastases. The urinary excretion rate was determined in 6 urine samples of each patient collected over 48 h at 8-h intervals beginning immediately after the administration of ^{188}Re-HEDP. After injection of ^{188}Re-HEDP, blood samples were taken weekly for 6 wk, and platelet and leukocyte counts were performed. **Results:** The mean effective half-life was 15.9 ± 3.5 h in bone metastases, 10.9 ± 2.1 h in the bone marrow, 11.6 ± 2.1 h in the whole body, 12.7 ± 2.2 h in the kidneys, and 7.7 ± 3.4 h in the bladder. The following radiation-absorbed doses were calculated: 3.83 ± 2.01 mGy/MBq for bone metastases, 0.61 ± 0.21 mGy/MBq for the bone marrow, 0.07 ± 0.02 mGy/MBq for the whole body, 0.71 ± 0.22 mGy/MBq for the kidneys, and 0.99 ± 0.18 mGy/MBq for the bladder. ^{188}Re-HEDP showed a rapid urinary excretion within the first 8 h after therapy, with 41% of the ^{188}Re-HEDP administered being excreted. Forty-eight hours after therapy, the excretion rate was 60% ± 12%. Only 1 patient showed a decrease of platelet count below 100×10^9 counts/L. None of the patients presented with a decrease of leukocyte count below 3.0×10^9 counts/L. **Conclusion:** ^{188}Re-HEDP is an effective radiopharmaceutical used in the palliative treatment of metastatic bone pain. The radiation-absorbed dose is acceptable for bone pain palliation with low doses for the normal bone marrow and the whole body.

Key Words: radiation-absorbed dose; kinetics; ^{188}Re-hydroxyethylidene diphosphonate; bone metastases

J Nucl Med 2003; 44:953–960

Received Sep. 9, 2002; revision accepted Jan. 21, 2003.

For correspondence or reprints contact: Knut Liepe, MD, Department of Nuclear Medicine, University Hospital Dresden, Fetscherstrasse 74, 01307 Dresden, Germany.

E-mail: liepe@rcs.urz.tu-dresden.de

The skeleton is a frequent site for metastases in prostate and breast cancer. Resulting bone pain interferes with the patient's quality of life and requires effective treatment. Unfortunately, various nonradiotherapeutic modalities—such as analgesics, hormone therapy, orchidectomy, cytostatic and cytotoxic drugs, bisphosphonates, and surgery—are not effective especially in the late stages of the disease. External-beam radiotherapy is suitable only for well-defined localized bone metastases. Extended field radiation may be useful in patients with diffuse metastases but is often accompanied by serious side effects. Therefore, systemic radionuclide therapy must be taken into consideration as a valuable and effective method of treatment of patients with widespread skeletal metastases.

The various radiopharmaceuticals that are used for palliative treatment of bone metastases include ^{89}Sr, ^{32}P, ^{131}I-α-amino-(4-hydroxybenzylidene)-diphosphonate, ^{90}Y, ^{186}Re-hydroxyethylidene diphosphonate (^{186}Re-HEDP), and ^{153}Sm-ethylenetriaminetetramethylene phosphonate (^{153}Sm-EDTMP). More recently, ^{117m}Sn-diethylenetriaminepentaacetic acid, ^{188}Re-HEDP, and ^{188}Re-dimercaptosuccinic acid have been reported to be effective for bone pain palliation.

For >4 y, we performed therapy with ^{188}Re-HEDP for the palliative treatment of bone metastases. The favorable physical characteristics of the radionuclide for its use in palliative therapy are a short physical half-life of 16.8 h and a maximal β-energy of 2.1 MeV with a 15% γ-component of 155 keV. This γ-component allows the determination of tissue distribution of the radiopharmaceutical for dosimetric calculations.

High skeletal accumulation of ^{188}Re-HEDP and rapid renal excretion maximally at 1 h after injection were found in animal experiments (*1*). The biologic half-life was 60.9 h in bone, 2.99 h in muscle tissue, and 6.21 h in blood (*1*).

For calculations of radiation-absorbed doses, it is necessary to take into consideration the complexity of osseous tissue consisting of cortical and trabecular structures as well as bone marrow. Cortical bone consists of central haversian canals lined with a layer of endosteum and surrounded by

bone lamellae. Trabecular bone is formed as a complex network of bone trabeculae and tissue cavities (*2*). Osteogenic cells are found on the surface of the trabecular bone cavities and line the haversian canals within cortical bone (*3*).

Normal bone remodeling is a balance between the resorptive activity of osteoclasts and the bone-forming function mediated primarily by osteoblasts (*4*). Phosphorus compounds are able to accumulate in the organic part of bone tissue (*5*) followed by a strong binding on hydroxyapatite crystals (*6*). The uptake of radiolabeled compounds such as ^{188}Re-HEDP depends on 2 factors, the local blood flow and the rate of osteogenesis (*7*).

The local effects of bone metastases result in increased bone destruction (osteolysis), reactive increase in bone formation (osteosclerosis), or both (*8*), suggesting that the physiologic processes of resorption and formation in normal bone are not completely lost in bone metastases.

Reformation of bone takes place within or around metastases; therefore, often a uniform lesion model is used for macroscopic level dose calculations (*9,10*). Using this model, the following assumptions are made (*11*): (a) the morphology of the lesion is homogeneous, (b) the distribution of radioactivity within the lesion is uniform, and (c) the energy emitted by decay of the radionuclide is >90% (*12*) deposited within the lesion if the diameter is >15 mm (*13*). As an alternative method, the surface model was used, with the assumption of a distribution on the surface up to a depth of 1 μm of a lesion (*9–11*). In this context, Maxon et al. (*10*) described a higher radiation-absorbed dose in the lesion using the surface model in comparison with the uniform model.

The major dose-limiting factor for radionuclide therapy is bone marrow toxicity, which results in a reduction in peripheral blood count, especially counts of platelets. The absorbed dose to the bone marrow from radionuclides incorporated in the bone has 4 sources: (a) radioactivity within the blood and extracellular fluid (*14*) of the marrow, (b) radioactivity fixed to the endosteum, (c) radioactivity in the bone matrix, and (d) radioactivity in all other surrounding organs (*15*). Because most of the radiopharmaceuticals used in bone palliation therapy localize predominantly in the skeletal tissues and emit primarily high-energy β-particles, the marrow absorbed dose results mainly from (b) and (c) (*15*).

We determined the kinetics and calculated the radiation-absorbed dose for ^{188}Re-HEDP using the uniform lesion model.

MATERIALS AND METHODS

Preparation of ^{188}Re-HEDP

^{188}Re-HEDP was prepared as described by Lin et al. (*1*) and Palmedo et al. (*16*). ^{188}Re-Perrhenate was obtained from a 38-GBq alumina-based ^{188}W/^{188}Re generator (*17*) (Oak Ridge National Laboratory). The generator was eluted with 20–25 mL of 0.9% saline. The generator eluates were concentrated to about 1.2 mL using a tandem cation/anion concentration system (*18*), which consists of an Ag Plus cartridge (Alltech Associates) attached to a 3-way stopcock connected at the outlet to the QMA anion-trapping SepPak (Waters Corp.) anion-exchange column. The concentration system was housed in an acrylic shield.

Kit vials were used to weigh 8.3 mg of HEDP (Fluka Chemie AG), 3.0 mg of gentisic acid (Sigma-Aldrich), and 3.9 mg of stannous chloride dihydrate (Merck), which were mixed with 1.0 mL of carrier-added ^{188}Re-generator eluate (10 μL $HReO_4$ [Aldrich], 100 μmol/mL physiologic saline). The solution was heated at 96°C–100°C for 15 min. After cooling to room temperature, 1 mL of sterile 0.3 mol/L NaOH solution was added to adjust the pH to 5–6.

Quality control of carrier-added ^{188}Re-HEDP was performed with thin-layer chromatography (TLC) using silica gel (ITLC-SG) strips (Gelman). In addition, anion-exchange chromatography was performed based on gradient elution with increasing concentrations of NaCl solutions using a QMA SepPak column. The radiochemical purity determined by both procedures (ITLC and ion exchange) was >90%.

Sterility and pyrogen tests were performed on each preparation.

Patient Selection

Eighteen male patients (mean age, 67 y; range, 56–87 y) with disseminated bone metastases from prostate cancer received a single intravenous injection of ^{188}Re-HEDP (range, 2,700–3,459 MBq; mean dose, 3,120 ± 419 MBq). The data from 5 of the 18 patients could not be included because complete gamma-camera scan data were not obtained, reducing the number of patients investigated to 13.

Chemotherapy and bisphosphonate therapy were discontinued 8 wk before the radiopharmaceutical injection. In accordance with the Helsinki Declaration, all patients were informed comprehensively about the study and possible side effects and were provided with a leaflet. Approval was obtained from the local ethics committee.

Study Design

All patients were hospitalized for 48 h. ^{188}Re-HEDP was administered as a bolus injection followed by flushing with physiologic saline. In 13 patients, anterior and posterior whole-body images were obtained using a dual head, large-field-of-view gamma camera (Genesys; ADAC Laboratories) at 3, 20, and 28 h after injection of ^{188}Re-HEDP. A 10% window was centered around a peak of 155 keV, and the camera was moved with a speed of 15 cm/min. We used high-energy collimators to reduce the effect of the bremsstrahlung to the image quality. The whole body was scanned, together with a standard of ^{188}Re-HEDP in a lead and acrylic container. Nine patients underwent a posttherapeutic SPECT scan at 19 h to determine the volume of bone metastases. After reconstruction, each dataset was sectioned at 1-pixel (0.68 cm) intervals along the transverse and coronal planes. A 64 × 64 matrix was used. Calculations were then performed directly on the reconstructed data (*19*). We delineated the perimeter of the lesions of SPECT data (Figs. 1 and 2) with a threshold of 43% (*20*) in all slices in which we could visualize the lesions. The volume of bone metastases was calculated based on the number of voxels with a threshold of 43%. Evaluation of the posttherapeutic data was performed by only 1 investigator to avoid interobserver variability. The nodule module of MIRDOSE3.1 was available only for spheric volumes. The differences between spheric and ellipsoid geometry in absorbed energy were ignored because of the relative

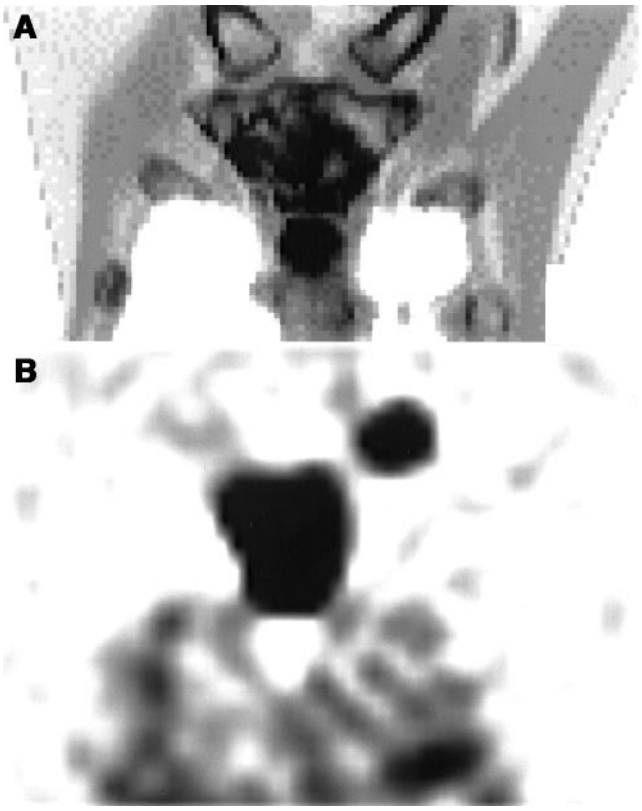

FIGURE 1. Example of large osteoblastic bone metastases in corpus sterni. (A) Visualization of metastases by coronal slice of CT. (B) Visualization of metastases by coronal slice of ^{188}Re-HEDP SPECT.

large volume of the investigated bone metastases (all diameters of bone metastases, >15 mm (*13*)). Thus, we assumed that the greater part of the energy would be deposited in the bone metastases. In an additional 5 patients with 11 bone metastases, we compared our volume determinations using SPECT data with the volumes estimated using CT. We found a deviation of 19% ± 10% between the 2 methods; the maximal deviation was 32% (Table 1).

Total whole-body counts were calculated as a geometric mean using the anterior and posterior scans. To determine the fraction of the injected activity in metastases as well as in the whole skeleton, kidneys, and bladder, background-corrected counting rates measured in regions of interest (ROIs) over metastases and various organs were divided by the background-corrected counts of the standard. The results were related to the administered dose. Thereby, a calculation of the ^{188}Re uptake in the percentage injected dose (%ID) in the whole body, metastases, and organs was performed in 13 patients. For 4 patients without SPECT data, we calculated only the radiation-absorbed dose of the whole body, bone marrow, kidney, and bladder.

For determination of the blood clearance curve, serial blood samples were collected in heparinized tubes from each patient over 6 h at 1-h intervals and also after 20 and 28 h following therapy to determine the activity in the blood. The total activity in the blood pool was normalized as a percentage of the injected activity. Pooled urine samples were collected at 0–8, 8–16, 16–24, 24–32, 32–40, and 40–48 h after ^{188}Re-HEDP administration to measure the total body clearance by urinary excretion. To determine any bone marrow impairment, leukocyte and platelet counts were determined weekly for 6 wk. A 12-wk blood count was obtained to show late effects or, conversely, improvement after an initial depression.

Calculations to determine the absorbed dose were performed using the MIRD schema. The effective half-life ($t_{1/2_{eff}}$) was determined from the fitted time–activity curve (activity as a percentage of the administered dose) in the ROI by the least-squares method assuming a monoexponential uptake function. The residence time was calculated from the area under the time–activity curve. The residence time (τ_j) is the ratio of the cumulated activity ($\tilde{A}$) and the administered activity (A_0) (*21*):

$$\tau_j = \tilde{A}/A_0.$$

The cumulated activity ($\tilde{A}$) is defined as the time integral of $A_h(t)$ (activity in a specific ROI over time) (*21*):

$$\tilde{A} = \int_0^\infty A_h(t)dt.$$

The activity in bone was determined using the following equation:

$$A_{bone}(t) = A_0 - (A_{collected\ urine}(t) + A_{blood}(t) + A_{kidney}(t) + A_{bladder}(t)),$$

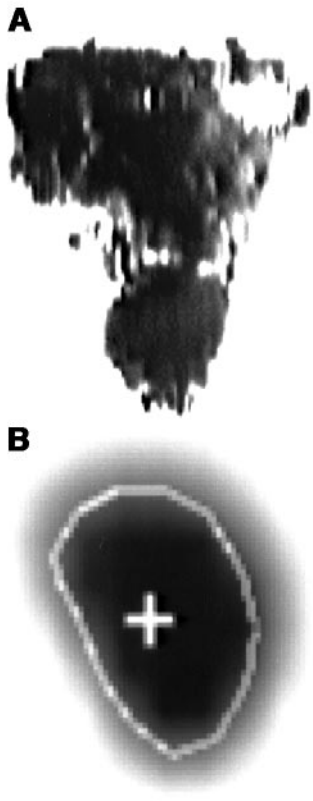

FIGURE 2. Example for volume estimation in same bone metastases as in Figure 1. (A) Volume estimation of metastases by multiplying thickness of each slice by sum of areas enclosed by boundaries. (B) Volume estimation of metastases by number of voxels enclosed by boundaries with threshold of 43%.

TABLE 1
Calculation of Volume of 11 Bone Metastases in 5 Patients Using SPECT Data (Delineation of Perimeter of Lesion with Threshold of 43%) and CT Data

Patient no.	Metastases* (*n*)	Volume		Radiation dose		Deviation‖ (%)
		Using CT† (mL)	Using SPECT‡ (mL)	Using CT§ (mGy/MBq)	Using SPECT¶ (mGy/MBq)	
1	1	16	22	5.92	4.28	29
	2	22	20	2.43	2.66	9
2	3	70	52	1.98	2.63	25
	4	44	36	2.46	2.98	8
3	5	59	58	4.89	4.97	2
4	6	24	17	4.77	6.42	27
	7	19	14	4.42	5.92	26
	8	44	64	1.97	1.36	32
	9	46	40	3.15	3.63	13
5	10	58	51	4.28	4.90	12
	11	30	33	2.87	2.60	10

*Number of bone metastases.
†Volume estimation using CT data.
‡Volume estimation using SPECT data.
§Calculation of radiation-absorbed dose in bone metastases using volume determined by CT data.
¶Calculation of radiation-absorbed dose in bone metastases using volume determined by SPECT data.
‖Deviation of volume estimation and calculation of absorbed dose between 2 methods using CT data and SPECT data.

where $A_{bone}(t)$ is activity in the bone as a function of time, $A_{collected\ urine}(t)$ is activity in the urine samples within 48 h from 0 to t, $A_{blood}(t)$ is activity in the blood samples at time t, $A_{kidney}(t)$ is activity in the kidneys at time t, and $A_{bladder}(t)$ is activity in the bladder at time t.

With the MIRD schema (*21*), we calculated the radiation-absorbed dose:

$$D_k = A_0 \Sigma_j \tau_j \times S_j(r_k \leftarrow r_j),$$

where $S_j(r_k \leftarrow r_j)$ is the S value, the mean absorbed dose per unit accumulated activity with j as the source and k as the target.

The distribution of the radionuclide in the metastases was assumed to be homogeneous. The volume and residence time data were entered into the nodule module option of the MIRDOSE3.1 program (*22*) to obtain the specific radiation-absorbed dose values for assumed soft-tissue tumors. This calculation was performed for 29 bone metastases.

For estimation of the radiation-absorbed dose to the bone marrow we considered 3 sources of radiation: (a) trabecular bone, (b) cortical bone, and (c) activity in bone marrow. According to the International Commission on Radiological Protection (ICRP) (*23*), an equal distribution of the radionuclide to trabecular and cortical bone was assumed. The activity in the bone marrow was determined by multiplying the activity concentration in blood by the blood volume of bone marrow. A value of 100 mL was assumed as a standard blood volume of bone marrow, in accordance with ICRP Publication 70 in Reference Man (*24*), which also fits with the data of Sgouros (*14*). A more precise model for radiolabeled antibody therapies is designed by Sgouros (*25*), including the determination of marrow-rich regions with different marrow kinetics.

RESULTS

The kinetic data of ^{188}Re-HEDP for 13 patients are shown in Figures 3–5. The %ID values for the whole body, the skeleton, and the bone metastases are corrected for physical half-life. The urinary excretion of ^{188}Re-HEDP is rapid within the first 8 h and, after 48 h, 60 ± 12 %ID of the ^{188}Re-HEDP was excreted (Fig. 3). The whole-body retention is shown to be roughly inverse to the cumulated urine activity (Fig. 4). The decay-corrected whole-body activity expressed as the percentage of the applied uptake of the whole body decreased quickly (Table 2). In contrast, the decrease of the decay-corrected activity in bone metastases was slow (Fig. 5). The biologic half-life ($t_{1/2_{biol}}$) was 51 ± 43 h in the whole body compared with a $t_{1/2_{biol}}$ of 269 ± 166 h in bone metastases (Table 3). The decrease of activity in the skeleton was also slow (Fig. 4). We found a longer $t_{1/2_{eff}}$ in bone metastases (15.9 ± 3.5 h) in comparison with the whole body (11.6 ± 2.1 h) ($P = 0.0010$) (Table 3).

The specific radiation-absorbed dose values in several critical organs were calculated from the described equations (*21*,*22*) using MIRDOSE3.1. The results are summarized in

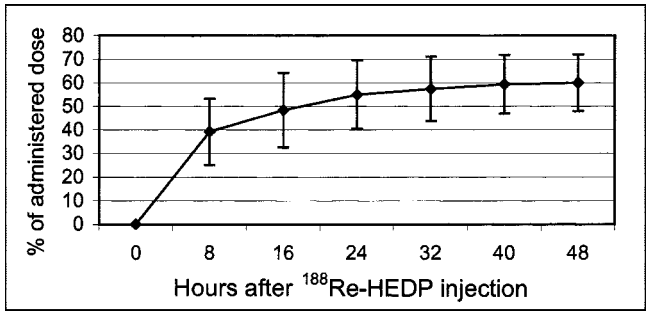

FIGURE 3. Decay-corrected cumulative excretion rate in urine after ^{188}Re-HEDP administration.

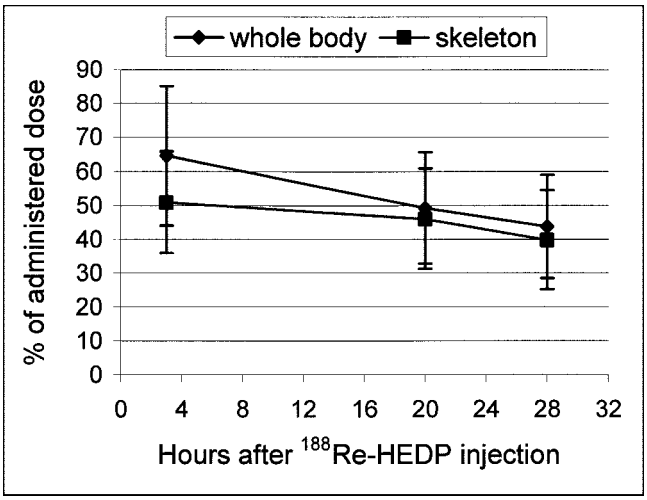

FIGURE 4. Decay-corrected percentage uptake value of ^{188}Re-HEDP in whole body (♦) and in skeleton (■).

Table 3. The mean specific radiation-absorbed dose in bone metastases (3.83 ± 2.01 mGy/MBq) was 6–7 times higher than the dose in bone marrow (0.61 ± 0.21 mGy/MBq). Because of the rapid urinary excretion rate, the radiation-absorbed dose to the whole body was low (0.07 ± 0.02 mGy/MBq).

The bone marrow toxicity of ^{188}Re-HEDP was assessed by the percentage change in platelet counts. A mean decrease of 30% ± 14% from the initial value before therapy was seen, maximally at 2.7 ± 0.9 wk (Fig. 6). Only 1 patient showed a decrease below 100 × 10^9/L and the nadir was 88 × 10^9/L (thrombocytopenia grade I according to the World Health Organization (*26*)). The leukocyte counts showed a mean decrease of 25% ± 17% from the value before therapy (Fig. 7), with a maximum at 3.0 ± 0.6 wk. In no case was a decrease of leukocyte counts below 3.0 × 10^9/L found (the borderline to leukopenia grade I according to the World Health Organization). In all patients, platelet and leukocyte counts returned to baseline levels within 12 wk after ^{188}Re-HEDP administration.

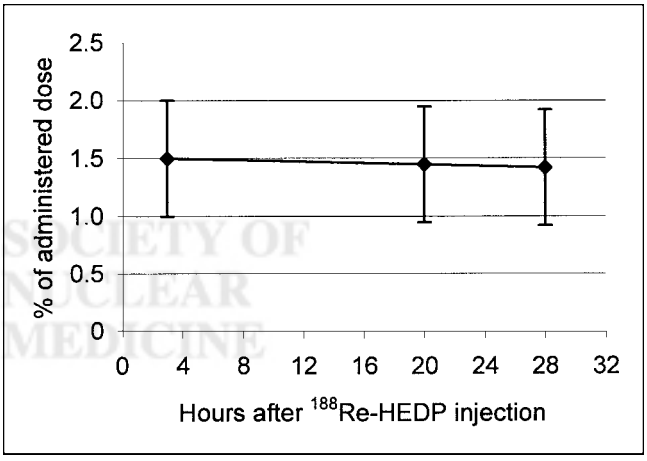

FIGURE 5. Decay-corrected percentage uptake value of ^{188}Re-HEDP in bone metastases.

TABLE 2
Decay-Corrected Percentage Uptake Value of Administered ^{188}Re-HEDP in Whole Body, Skeleton, and Bone Metastases of 13 Patients

Uptake	Time after administration		
	3 h*	20 h*	28 h*
Whole body (%)	64.6 ± 20.5	49.3 ± 16.4	43.8 ± 15.2
Skeletal (%)	50.9 ± 14.9	46.1 ± 14.8	39.9 ± 14.6
Bone metastases (%)	1.51 ± 0.57	1.45 ± 0.68	1.42 ± 0.56

*Time after therapy.

DISCUSSION

A uniform lesion model for the calculation of bone absorbed radiation dose is frequently used (*9–10*). The prerequisite for such a model is a uniform distribution of radioactivity within the bone. However, ^{188}Re-HEDP seems to be taken up to a greater extent at the surface of the bone or in bone metastases rather than by the rest of the normal bone. Therefore, the assumption of a homogeneous distribution of ^{188}Re-HEDP might not accurately match reality and could influence the results of the calculated absorbed dose in metastases. Breen et al. (*27*) described a 2-component model of an osteoblastic metastatic lesion containing bone and soft tissue. The radioisotope is assumed to reside only within the bone, but metastatic cells are also present within the soft tissue. The limitations of the uniform model are therefore evident. More recently, Samaratunga et al. (*11*) have reported a heterogeneous lesion dosimetry model, based on Monte Carlo simulations with data from histomorphometry of ^{186}Re-HEDP distribution in bone lesions. In this model, it is assumed that the ^{186}Re-HEDP is deposited on the bone surface and bone spicules to a depth of 10 μm. Nevertheless, in this study we used the uniform lesion model because no other model was available. Furthermore, a problem for dosimetry is the determination of the volume of the bone metastases. In various studies, CT images were used for the determination of lesion volumes (*10,28*). In our hospital, high-resolution CT was not available in the early phase of our study and, thus, partial-volume effects were present within the images. Therefore, we used posttherapy SPECT data for the delineation of the volume of bone metastases. The differences between the volume estimation by CT and SPECT were explainable by the application of a morphologic method and the visualization of the bone turnover. We designed an elliptic model from the SPECT data and calculated the volume. This volume were equated with a spheric volume to meet the demands of the MIRDOSE algorithm. In an additional 5 patients, we estimated a mean radiation-absorbed dose for bone metastases of 3.8 ± 1.3 mGy/MBq using SPECT data and of 3.6 ± 1.2 mGy/MBq

TABLE 3
Radiation-Absorbed Dose, $t_{1/2_{eff}}$, and Residence Time in 29 Bone Metastases, in Bone Marrow, Whole Body, Kidneys, and Bladder of 13 Patients

Parameter	Bone metastases	Red bone marrow	Whole body	Kidneys	Bladder
Radiation-absorbed dose* (mGy/MBq)	3.83 ± 2.01	0.61 ± 0.21	0.07 ± 0.02	0.71 ± 0.22	0.99 ± 0.18
$t_{1/2_{eff}}$	15.9 ± 3.5	10.9 ± 2.1	11.6 ± 2.1	12.7 ± 2.2	7.7 ± 3.4
$t_{1/2_{biol}}$	269 ± 166	36 ± 20	51 ± 43	75 ± 67	18 ± 15
Residence time (h)	0.16 ± 0.20	10.61 ± 2.43	11.08 ± 2.86	0.42 ± 0.15	0.23 ± 0.15

*Radiation-absorbed dose per unit administered activity.

using CT data (maximum deviation of 1.36 mGy/MBq using SPECT data to 1.97 mGy/MBq using CT data).

We found the $t_{1/2_{eff}}$ of ^{188}Re (15.9 ± 3.5 h) to be longer in bone metastases than in the whole body (11.6 ± 2.1 h). These results correspond to the data of Lee et al. (*29*), who found a half-life of 16.4 ± 1.7 h in bone metastases and only 12.5 ± 1.8 h in the whole body and an absorbed radiation dose value of 14.6 ± 1.85 Gy (4.9 ± 0.6 mGy/MBq) in bone metastases. Similar to these results, we estimated a high radiation-absorbed dose to bone metastases with a mean value of 12.4 ± 6.2 Gy (3.83 ± 2.01 mGy/MBq) and a broad range in the various single metastases from 5.3 to 31.3 Gy for a mean activity of 3,120 MBq ^{188}Re-HEDP (Table 3). This value is lower compared with that of other investigators—for example, for ^{186}Re-HEDP (*30*) with a mean radiation-absorbed dose for bone metastases of a median value of 26 Gy. An inaccuracy of the dose estimation is due to the limitation in the MIRDOSE3.1 nodule module, which is only valid for spheric volumes and soft tissue (water). In addition, MIRDOSE3.1 uses only the mean β-energy, not the full β-spectrum. Also, the bremsstrahlung is neglected, but this caused only an error of <1% (*12*). The activity in bone metastases was underestimated because we used no attenuation correction. This correction requires transmission studies and is not widely used (*25*).

In comparison with the calculated radiation-absorbed doses in the various patients, we found no uniform values within 1 patient, as 1 patient showed bone metastases with higher and lower radiation-absorbed doses. In addition, we could not find a relation between a good response (defined as pain relief ≥25% on the visual analog scale at least in 2 consecutive weeks without increase of analgesics intake) and the amount of the radiation-absorbed dose in the metastases.

Lin et al. (*1*) described a low uptake of radioactivity and a rapid washout from the muscle tissue and blood after intravenous administration of ^{188}Re-HEDP to laboratory animals. These results correspond with our human data of a low radiation-absorbed dose of 0.22 ± 0.05 Gy (0.07 ± 0.02 mGy/MBq) in the whole body. These differences between radiation-absorbed doses in the bone metastases and the whole body seem favorable for getting a satisfactory therapeutic effect using ^{188}Re-HEDP with a low radiation exposure to the whole body. This assumption is supported by the effect of the ^{188}Re-HEDP therapy showing an average palliation for bone pain in 80% of our patients (*31*).

In both animal studies and investigations in 5 prostate cancer patients with administration of 178–185 MBq ^{188}Re-HEDP, radiation-absorbed doses of 0.37 ± 0.06 cGy/37 MBq for the whole body were calculated by Maxon et al.

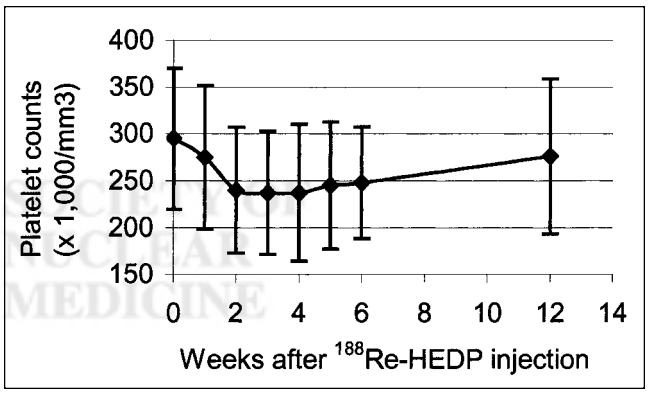

FIGURE 6. Bone marrow impairment from ^{188}Re-HEDP expressed as platelet counts in serial blood samples for about 6 wk.

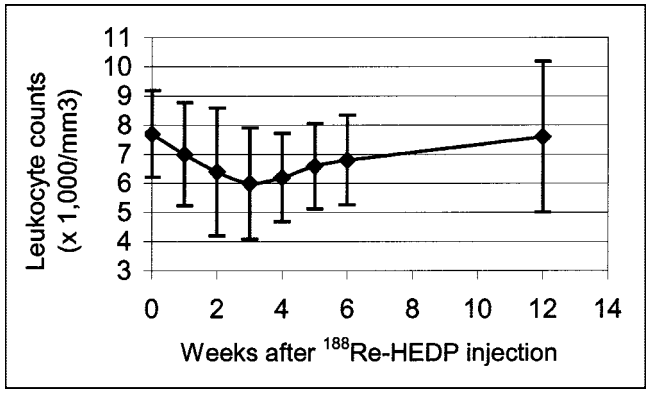

FIGURE 7. Bone marrow impairment from ^{188}Re-HEDP expressed as leukocyte counts in serial blood samples for about 6 wk.

(*32*). These values correspond to a radiation-absorbed dose in the whole body of 0.07 ± 0.02 mGy/MBq (0.26 cGy/37 MBq) in our study. Furthermore, Maxon et al. (*32*) calculated a radiation-absorbed dose of 5.2 ± 1.2 cGy/37 MBq for the kidneys, 3.6 ± 1.1 cGy/37 MBq for the bladder wall, and 3.5 ± 0.7 cGy/37 MBq for the red bone marrow. However, we observed lower radiation-absorbed doses: in the kidneys, 0.71 mGy/MBq (2.6 cGy/37 MBq); in the bladder wall, 0.99 mGy/MBq (3.7 cGy/37 MBq); and in the red bone marrow, 0.61 mGy/MBq (2.3 cGy/37 MBq).

Our data showed a similar dose for the bone marrow comparison with other bone-seeking radionuclides with lower β-energies than ^{188}Re-HEDP. For 1,285 MBq ^{186}Re-HEDP, the dose was 1.73 Gy (*30*) and, for 37–111 MBq/kg body weight ^{153}Sm-EDTMP, the dose ranged from 1.27 to 2.25 Gy (*33*), in consideration to the longer physical half-life and the lower activity used, compared with ^{188}Re-HEDP. The hematologic toxicity of ^{188}Re-HEDP is also similar to results achieved with ^{186}Re-HEDP (*34*,*35*). In radiolabeled antibody therapy, Sgouros et al. (*25*) described a more precise model for calculation of red bone marrow using biopsy and dividing the marrow kinetic in different marrow-rich regions. However, in therapies with bone-seeking radiopharmaceuticals, the bone uptake is the dominant factor for the bone marrow dose.

^{188}Re-HEDP is excreted mainly by the urinary system. Maxon et al. (*10*) found that for ^{186}Re-HEDP there is a rapid urinary excretion rate of 45% within the first 5 h, and Graham et al. (*9*) described a urinary excretion rate of 42% within the first 3 h. Lin et al. (*1*) found an excretion rate of 51% of the injected ^{188}Re-HEDP within 4 h after therapy and 60% within 24 h in rats. In 23 patients with bone metastases, a urinary excretion of 62% was seen within 5 d for ^{188}Re-HEDP (*36*). This value is comparable to the urinary excretion rate of 63% ± 13% within 48 h calculated in our study.

CONCLUSION

The high uptake of ^{188}Re-HEDP and the long $t_{1/2_{biol}}$ in bone metastases result in a high mean radiation-absorbed dose of 3.8 ± 2.0 mGy/MBq. The mean radiation-absorbed dose to the whole body of 0.07 ± 0.02 mGy/MBq is low because of the rapid urinary excretion of the radionuclide. A mean dose value of 0.6 ± 0.2 mGy/MBq for the red bone marrow did not lead to any clinically significant thrombocytopenia or leukopenia. The results of our studies demonstrate that ^{188}Re-HEDP is a new and less-expensive alternative agent for the bone pain palliation. Further studies should be directed to the use of a heterogeneous lesion model. It seems to be important to detect the deviation between the results for radiation-absorbed doses obtained by different models for the distribution of radioactivity within the bone.

ACKNOWLEDGMENTS

Research at the Oak Ridge National Laboratory was supported by the U.S. Department of Energy under contract DE-AC05-00OR22725 with UT-Battelle, LLC.

REFERENCES

1. Lin W, Lin C, Yeh S, et al. Rhenium-188 HEDP: a new generator-produced radiotherapeutic drug of potential value for treatment of bone metastases. *Eur J Nucl Med.* 1997;24:590–595.
2. Bouchet LG, Jokisch DW, Bolch WE. A three-dimensional transport model for determining absorbed fraction of energy for electrons within trabecular bone. *J Nucl Med.* 1999;40:1947–1966.
3. Bouchet LG, Bolch WE. A three-dimensional transport model for determining absorbed fraction of energy for electrons within cortical bone. *J Nucl Med.* 1999;40:2115–2124.
4. Scher HI, Chung L. Bone metastases: improving the therapeutic index. *Semin Oncol.* 1994;21:630–656.
5. Rohlin M, Hammerström L. Distribution of ^{99m}Tc-labelled phosphorus compounds ^{45}Ca and ^{85}Sr in diphosphonate-treated rats. *Acta Radiol.* 1977;16:513–524.
6. Subramanian G, McAfee JG, Blair RJ, Mether A, Connor T. ^{99}Tc-EHDP: a potential radiopharmaceutical for skeletal imaging. *J Nucl Med.* 1972;13:947–950.
7. Christensen SB, Krogsgaard OW. Localization of Tc-99m MDP in epiphyseal growth plates of rats. *J Nucl Med.* 1981;22:237–245.
8. Nielsen O, Munro A, Tannock I. Bone metastases: pathophysiology and management policy. *J Clin Oncol.* 1991;3:509–524.
9. Graham M, Scher H, Liu GB, Yeh S, Curley T. Rhenium-186-labeled hydroxyethylidene diphosphonate dosimetry and dosing guidelines for the palliation of skeletal metastases from androgen-independent prostate cancer. *Clin Cancer Res.* 1999;5:1307–1318.
10. Maxon HR, Deutsch EA, Thomas SR, et al. Re-186(Sn) HEDP for treatment of multiple metastatic foci in bone: human biodistribution and dosimetric study. *Radiology.* 1988;166:501–507.
11. Samaratunga RC, Thomas SR, Hinnefeld JD, et al. A Monte Carlo simulation model for radiation dose to metastatic skeletal tumor from rhenium-186(Sn)-HEDP. *J Nucl Med.* 1995;36:336–350.
12. Siegel JA, Stabin MG. Absorbed fraction for electrons and beta particles in spheres of various sizes. *J Nucl Med.* 1994;35:152–156.
13. Sarfaraz M, Wessels BW. Validation of an analytical expression for the absorbed dose from a spherical beta source geometry and its application to micrometastatic radionuclide therapy. *Clin Cancer Res.* 1999;5:3020s–3023s.
14. Sgouros G. Bone marrow dosimetry for radioimmunotherapy: theoretical considerations. *J Nucl Med.* 1993;34:689–694.
15. Goddu SM, Bishayee A, Bouchet LG, Bolch WE, Rao DV, Howell RW. Marrow toxicity of ^{33}P- versus ^{32}P-orthophosphate: implications for therapy of bone pain and bone metastases. *J Nucl Med.* 2000;41:941–951.
16. Palmedo H, Guhlke S, Bender H, et al. Dose escalation study with rhenium-188 hydroxyethylidene diphosphonate in prostate cancer patients with osseous metastases. *Eur J Nucl Med.* 2000;27:123–130.
17. Knapp FF Jr, Beets AL, Guhlke S, et al. Development of the alumina-based tungsten-188/rhenium-188 generator and use of rhenium-188-labeled radiopharmaceutical for cancer treatment. *Anticancer Res.* 1997;17:1783–1796.
18. Guhlke S, Beets AL, Oetjen K, et al. Simple new method for effective concentration of ^{188}Re solutions from alumina-based ^{188}W-^{188}Re-generator. *J Nucl Med.* 2000;41:1271–1278.
19. Zanzonico PB, Bigler RE, Sgouros G, Strauss A. Quantitative SPECT in radiation dosimetry. *Semin Nucl Med.* 1989;19:47–61.
20. Iosilevsky G, Israel O, Frenkel A, et al. A practical SPECT technique for quantitation of drug delivery to human tumors and organ absorbed radiation dose. *Semin Nucl Med.* 1989;19:33–46.
21. Fisher DR. Interpreting data from medical imaging for absorbed dose calculations. In: Handout Book of the 45th Annual Meeting of the Society of Nuclear Medicine; Toronto, Ontario, Canada; June 7–11, 1998:6–42.
22. Stabin MG. MIRDOSE: personal computer software for internal dose assessment in nuclear medicine. *J Nucl Med.* 1996;37:538–546.
23. International Commission on Radiological Protection. Limits for intakes of radionuclides by workers. *Ann ICRP.* 1979;30;1–58.
24. International Commission on Radiological Protection. Basic anatomical and

physiological data for use in radiobiological protection. Part 1. Skeleton. ICRP Publication 70. *Ann ICRP*. 1995;25:1–80.
25. Sgouros G, Stabin M, Erdi Y, et al. Red marrow dosimetry for radiolabeled antibodies that bind to marrow, bone, or blood components. *Med Phys.* 2000;27: 150–164.
26. World Health Organization. *WHO Handbook for Reporting Results of Cancer Treatment.* Geneva, Switzerland: World Health Organization. Offset publication. 1979;48:67–68.
27. Breen S, Battista J. Cavity theory applied to the dosimetry of systemic radiotherapy of bone metastases. *Phys Med Biol.* 2000;45:879–896.
28. Blake GM, Zivanovic MA, McEwan AJ, Batty VB, Ackery DM. ^{89}Sr radionuclide therapy: dosimetry and haematologic toxicity in two patients with metastasising prostatic carcinoma. *Eur J Nucl Med.* 1987;13:41–46.
29. Lee JS, Choi CW, Kim BI, et al. Evaluation of absorbed radiation dose of ^{188}Re-HEDP in patients with bone metastases using gamma camera [abstract]. *J Nucl Med.* 2000;5(suppl):239P.
30. Maxon HR, Schroder LE, Thomas SR, et al. Re-186(Sn)HEDP for treatment of painful osseous metastases: initial clinical experience in 20 patients with hormone resistant prostate cancer. *Radiology.* 1990;176:155–159.
31. Liepe K, Franke WG, Kropp J, Koch R, Runge R, Hliscs R. Comparison of rhenium-188-HEDP, rhenium-186-HEDP and strontium-89 in palliation of painful bone metastases. *Nuklearmedizin.* 2000;39:146–151.
32. Maxon H, Schroder L, Washburn L, Thomas S. Rhenium-188 (Sn) HEDP for treatment of osseous metastases. *J Nucl Med.* 1998;39:659–663.
33. Eary JF, Collins C, Stabin MG, et al. Samarium-153-EDTMP biodistribution and dosimetry estimation. *J Nucl Med.* 1993;34:1031–1036.
34. de Klerk JMH, van Dieren EB, van het Schip AD, et al. Bone marrow absorbed dose of rhenium-186-HEDP and the relationship with decreased platelet counts. *J Nucl Med.* 1996;37:646–651.
35. Sciuto R, Tofani A, Festa A, et al. Short- and long-term effects of ^{186}Re-1,1-hydroxyethylidene diphosphonate in the treatment of painful bone metastases. *J Nucl Med.* 2000;41:647–654.
36. Chen SL. Treatment of metastatic bone pain with ^{188}Re-HEDP [abstract]. *J Nucl Med.* 2000;5(suppl):265P.